JCTC Journal of Chemical Theory and Computation

pubs.acs.org/JCTC Article

Nonadiabatic Dynamics near Metal Surfaces with Periodic Drivings: A Generalized Surface Hopping in Floquet Representation

Yu Wang, Vahid Mosallanejad, Wei Liu, and Wenjie Dou*

Cite This: J. Chem. Theory Comput. 2024, 20, 644−650 Read Online

ACCESS | Metrics & More | Article Recommendations | Supporting Information

ABSTRACT: With light−matter interaction extending into the strong regime, as well as rapid development of laser technology, systems subjecting to a time-periodic perturbation have attracted broad attention. Floquet theorem and Floquet time-independent Hamiltonian are powerful theoretical frameworks to investigate the systems subjected to time-periodic drivings. In this study, we extend the previous generalized surface hopping (SH) algorithm near a metal surface (J. Chem. Theory Comput. 2017, 13, 6, 2430−2439) to the Floquet space, and hence, we develop a generalized Floquet representation-based SH (FR-SH) algorithm. Here, we consider an open quantum system with fast drivings. We expect that the present algorithm will be useful for understanding the chemical processes of molecules under time-periodic driving near the metal surface.

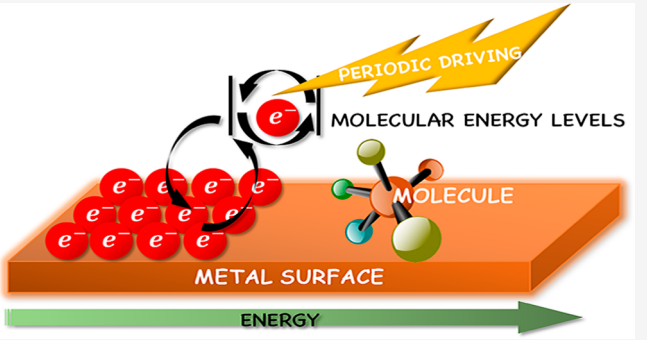

1. INTRODUCTION

The Born−Oppenheimer (BO) approximation is established based on the ratio of the mass of a nucleus to the mass of an electron so that nuclear motion is decoupled from electronic dynamics. However, when it comes to electronic excitation transfer or any form of electronic relaxation, BO dynamics break down such that one must take into account the coupling between the nuclear motion and electronic transitions.[1,2] When concerning molecule−metal interfaces, electrons from the metal are much easier to excite than for an isolated molecule, such that nonadiabatic dynamics are inevitable.[3] At molecule−metal interfaces, there are numerous chemical setups including heterogeneous catalysis,[4−6] chemisorption,[7,8] and molecular junctions.[9,10] For nonadiabatic dynamics, there are several numerical exact solutions, including numerical renormalization group (NRG) techniques,[11,12] multiconfiguration time-dependent Hartree (MCTDH),[13] hierarchical quantum master equation (HQME),[14,15] and quantum Monte Carlo (QMC).[16] However, these methods cannot deal with large degrees of freedom (DoFs) in a metal. Several years ago, Dou et al. developed a surface hopping (SH) algorithm near the metal surface which is based on a simple classical master equation (CME).[17,18] Such an SH algorithm treats all metallic electrons implicitly and works in the limit of weak molecule−metal interactions. For a realistic molecule with more than one orbital near the metal surface, Dou et al. developed a generalized SH algorithm in which the quantum−classical Liouville equation (QCLE) was embedded inside a CME.[19,20] In this study, we extend the generalized SH algorithm[20] to treat Floquet-engineered molecules near the metal surface.

Over the last few decades, advancements of high-power and short-pulse laser technologies have greatly facilitated the exploration of novel atomic and molecular properties.[21−23] It is also demonstrated that even without external light, vacuum fluctuations in the cavity can strongly couple with matter when electronic or vibrational transitions of the matter are resonant with the cavity mode.[24] Such strong light−matter interaction has been achieved to modify the nature of matter, resulting in novel properties including electronic conductivity,[25,26] energy transfer probability,[27,28] nonlinear optical response,[29−31] chemical reaction,[32,33] and so forth. It is thus necessary to theoretically investigate how matter properties can be modified by these strong external fields. As systems are subject to a strong time-periodic external stimulus, the standard nonlinear perturbation theory[34] becomes inaccurate. The Floquet theory is widely used in theoretical investigations, because it allows the reduction of the periodical or quasi-periodical time-dependent Schrödinger equation into a set of time-independent coupled equations.[35−37]

Received: November 16, 2023
Revised: December 27, 2023
Accepted: December 29, 2023
Published: January 10, 2024

Floquet-based nonadiabatic dynamics have been developed for both closed and open systems. For example, Schirò et al. developed a Floquet coupled-trajectory mixed quantum−classical (F-CT-MQC) algorithm for excited-state molecular dynamics simulations of systems subject to an external periodic drive.[38] Sato et al. employed the Maxwell−Bloch equation to investigate basic properties of nonequilibrium steady states of periodically driven open quantum systems.[39] Li et al. developed a Floquet engineering scattering formalism that relies on a systematic high-frequency expansion of the scattering matrix.[40] Fiedlschuster et al. used a Floquet-based SH algorithm to describe the dynamics of one positively charged hydrogen in strong field.[41] Nafari Qaleh et al. employed a Floquet master equation to study energy transfer from a quantum system to two thermal baths.[42] Chen et al. investigated different approaches to derive the proper Floquet-based QCLE (F-QCLE) for laser-driven electron−nuclear dynamics.[43] Wang et al. developed a Floquet SH and Floquet electronic friction for one level near the metal surface.[44,45] These Floquet-based methods have mainly been developed to deal with nonadiabatic dynamics in either closed quantum systems or open quantum systems coupled with bosonic baths. Notably, few approaches for Floquet-based nonadiabatic dynamics have been developed for open quantum systems with Fermionic baths. Therefore, our objective is to develop a Floquet-based method to treat nonadiabatic dynamics near the metal surface (Fermionic bath) under periodic drivings.

In this study, we develop a generalized Floquet representation-based SH (FR-SH) algorithm near the metal surface in an extended Hilbert space. It is important to note that our FR-SH method is applicable under weak coupling conditions, namely, a temperature larger than the system−bath coupling.

We organize the paper as follows: in Section 2, we introduce the FR-QCLE-CME and FR-SH algorithm. In Section 3, we discuss the results of FR-SH and FR-QME. We conclude in Section 4.

2. THEORY

2.1. Equation of Motion in FR. To be explicit, we divide the general total Hamiltonian into three parts: the system H_s that is driven by external drivings, the bath H_b, and the system−bath coupling H_c

$$\hat{H}(t) = \hat{H}_s(t) + \hat{H}_b + \hat{H}_c \tag{1}$$

$$\hat{H}_s(t) = \sum_{ij} h_{ij}(\hat{\boldsymbol{R}}, t)\hat{d}_i^{+}\hat{d}_j + U_0(\hat{\boldsymbol{R}}) + \sum_{\alpha} \frac{\hat{\boldsymbol{P}}_\alpha^2}{2m_\alpha} \tag{2}$$

$$\hat{H}_b = \sum_k \epsilon_k \hat{c}_k^{+}\hat{c}_k \tag{3}$$

$$\hat{H}_c = \sum_{ki} V_{ik}(\hat{c}_k^{+}\hat{d}_i + \hat{d}_i^{+}\hat{c}_k) \tag{4}$$

Here, $\hat{d}_i^{+}(\hat{d}_i)$ is the creation (annihilation) operator for the i-th electronic orbital of the molecule; $\hat{c}_k^{+}(\hat{c}_k)$ is the creation (annihilation) operator for the k-th electronic orbital of the metal surface. $\hat{\boldsymbol{R}}$ and $\hat{\boldsymbol{P}}$ are nuclear positions and momenta, respectively (α represents the DoF of nuclei). m_α is the nuclear mass. $U_0(\hat{\boldsymbol{R}})$ is the diabatic nuclear potential for the unoccupied state. We consider a system under the periodic driving so that $h_{ij}(\hat{\boldsymbol{R}}, t + T) = h_{ij}(\hat{\boldsymbol{R}}, t)$, where T is the driving period. V_{ik} is the coupling between the molecular orbital $\hat{d}_i$ and the metallic orbital $\hat{c}_k$. Under the wide band approximation, the hybridization function $\Gamma_{ij}(\epsilon)$ measures the strength of system−bath coupling which is independent of ϵ and is given by

$$\Gamma_{ij}(\epsilon) = 2\pi \sum_k V_{ik}V_{jk}\delta(\epsilon - \epsilon_k) = \Gamma_{ij} \tag{5}$$

To derive an equation of motion (EOM) with periodic driving, we first consider the case of no drivings, i.e., the total Hamiltonian is time-independent. Such that the EOM for the total density operator follows the Liouville−von Neumann (LvN) equation

$$\frac{\partial}{\partial t}\hat{\rho}(t) = -\frac{i}{\hbar}[\hat{H}, \hat{\rho}(t)] \tag{6}$$

Then, we can reduce the LvN equation to the Redfield equation in the weak system−bath coupling limit. In this regime, the EOM of the reduced system density operator $\hat{\rho}_s(t)$ is[19,20]

$$\frac{\partial}{\partial t}\hat{\rho}_s(t) = -\frac{i}{\hbar}[\hat{H}_s, \hat{\rho}_s(t)] - \hat{\hat{\mathcal{L}}}_{bs}\hat{\rho}_s(t) \tag{7}$$

here the superoperator $\hat{\hat{\mathcal{L}}}_{bs}$ includes information on system−bath couplings, which is

$$\hat{\hat{\mathcal{L}}}_{bs}\hat{\rho}_s(t) = \frac{1}{\hbar^2}\int_0^\infty d\tau\, e^{-i\hat{H}_s t/\hbar}\mathrm{Tr}_b ([\hat{H}_{Ic}(t), [\hat{H}_{Ic}(t-\tau), e^{i\hat{H}_s t/\hbar}\hat{\rho}_s(t) e^{-i\hat{H}_s t/\hbar} \otimes \hat{\rho}_b^{eq}]])e^{i\hat{H}_s t/\hbar} \tag{8}$$

where Tr_b indicates tracing over the bath (i.e., the metal surface) DoFs, and $\hat{\rho}_b^{eq}$ is the bath equilibrium density operators. Note that $\hat{H}_{Ic}(t)$ in the above equation is in the interaction picture, $\hat{H}_{Ic}(t) = e^{i(\hat{H}_s+\hat{H}_b)t/\hbar}\hat{H}_c e^{-i(\hat{H}_s+\hat{H}_b)t/\hbar}$. We refer to eq 7 as the QME.

For any periodic driving system, we can derive a Floquet LvN equation which describes the EOM in the FR.[46] Here, we follow ref 46 to construct Floquet Hamiltonian ($\hat{H}^F$). In the following, we briefly introduce two main operators, which are the Fourier number operators $\hat{N}$ and the Fourier ladder operators $\hat{L}_n$. They have the following properties

$$\hat{N}|n\rangle = n|n\rangle,\ \hat{L}_n|m\rangle = |n+m\rangle \tag{9}$$

where $|n\rangle$ is the basis set in the Fourier space. Then, the Hamiltonian and density operator in FR would be

$$\hat{H}^F = \sum_n \hat{H}^{(n)}\hat{L}_n + \hat{N}\hbar\omega \tag{10}$$

$$\hat{\rho}^F(t) = \sum_n \hat{\rho}^{(n)}(t)\hat{L}_n \tag{11}$$

where $\hat{H}^{(n)}$ and $\hat{\rho}^{(n)}(t)$ are the Fourier expansion coefficients in $\hat{H}(t) = \sum_n \hat{H}^{(n)}e^{in\omega t}$ and $\hat{\rho}(t) = \sum_n \hat{\rho}^{(n)}(t)e^{in\omega t}$. Here, n goes from $-\infty$ to ∞. Obviously (t) is Hermitian. Such that one can show that $\hat{H}^{-n} = (\hat{H}^n)^\dagger$. Note also that the ladder operator $\hat{L}_n$ follows the same relationship, $\hat{L}_{-n} = (\hat{L}_n)^\dagger$. In

https://doi.org/10.1021/acs.jctc.3c01263
J. Chem. Theory Comput. 2024, 20, 644−650

addition, the number operator $\hat{N}$ is Hermitian. Such that one can show the Floquet Hamiltonian $\hat{H}^{\mathrm{F}}$ is Hermitian. By employing such definitions, the EOM of $\hat{\rho}^{\mathrm{F}}(t)$ now reads as

$$\frac{\partial}{\partial t}\hat{\rho}^{\mathrm{F}}(t) = -\frac{i}{\hbar}[\hat{H}^{\mathrm{F}}, \hat{\rho}^{\mathrm{F}}(t)] \tag{12}$$

Correspondingly, the Redfield equation for the molecule density operator in FR $\hat{\rho}_{\mathrm{s}}^{\mathrm{F}}(t)$ reads as

$$\frac{\partial}{\partial t}\hat{\rho}_{\mathrm{s}}^{\mathrm{F}}(t) = -\frac{i}{\hbar}[\hat{H}_{\mathrm{s}}^{\mathrm{F}}, \hat{\rho}_{\mathrm{s}}^{\mathrm{F}}(t)] - \hat{\hat{\mathcal{L}}}_{\mathrm{bs}}^{\mathrm{F}}\hat{\rho}_{\mathrm{s}}^{\mathrm{F}}(t) \tag{13}$$

We refer to eq 13 as the QME in the FR (FR-QME).

We then proceed to perform a partial Wigner transformation for the density operator $\hat{\rho}_{\mathrm{s}}^{\mathrm{F}}(t)$, which is defined as

$$\hat{\rho}_{\mathrm{sW}}^{\mathrm{F}}(\boldsymbol{R}, \boldsymbol{P}, t) \equiv (2\pi\hbar)^{-N_\alpha}\int \mathrm{d}\boldsymbol{X}\langle \boldsymbol{R} - \boldsymbol{X}/2|\hat{\rho}_{\mathrm{s}}^{\mathrm{F}}(\hat{\boldsymbol{R}}, \hat{\boldsymbol{P}}, t) |\boldsymbol{R} + \boldsymbol{X}/2\rangle e^{i\boldsymbol{P}\cdot\boldsymbol{R}/\hbar} \tag{14}$$

where $\boldsymbol{R}$ and $\boldsymbol{P}$ can be interpreted as position and momentum variable in the classical limit instead of operators. $\boldsymbol{X}$ is the dummy variable. N_α is the number of nuclear DoFs. After performing a partial Wigner transformation for eq 13, we arrive at an FR-QCLE-CME

$$\begin{aligned}\frac{\partial}{\partial t}\hat{\rho}_{\mathrm{sW}}^{\mathrm{F}}(\boldsymbol{R}, \boldsymbol{P}, t) = &\frac{1}{2}\{\hat{H}_{\mathrm{sW}}^{\mathrm{F}}(\boldsymbol{R}, \boldsymbol{P}), \hat{\rho}_{\mathrm{sW}}^{\mathrm{F}}\} \\ &- \frac{1}{2}\{\hat{\rho}_{\mathrm{sW}}^{\mathrm{F}}, \hat{H}_{\mathrm{sW}}^{\mathrm{F}}(\boldsymbol{R}, \boldsymbol{P})\} \\ &- \frac{i}{\hbar}[\hat{H}_{\mathrm{sW}}^{\mathrm{F}}, \hat{\rho}_{\mathrm{sW}}^{\mathrm{F}}] - \hat{\hat{\mathcal{L}}}_{\mathrm{bsW}}^{\mathrm{F}}(\boldsymbol{R})\hat{\rho}_{\mathrm{sW}}^{\mathrm{F}}(t)\end{aligned} \tag{15}$$

here $\{\cdot, \cdot\}$ is the Poisson bracket

$$\{A, B\} = \sum_\alpha \left(\frac{\partial A}{\partial R_\alpha}\frac{\partial B}{\partial P_\alpha} - \frac{\partial A}{\partial P_\alpha}\frac{\partial B}{\partial R_\alpha}\right) \tag{16}$$

and $\hat{H}_{\mathrm{sW}}^{\mathrm{F}}$ indicates the partial Wigner transformation of $\hat{H}_{\mathrm{s}}^{\mathrm{F}}$. The superoperator $\hat{\hat{\mathcal{L}}}_{\mathrm{bsW}}^{\mathrm{F}}(\boldsymbol{R})$ in eq 15 becomes

$$\begin{aligned}&\hat{\hat{\mathcal{L}}}_{\mathrm{bsW}}^{\mathrm{F}}(\boldsymbol{R})\hat{\rho}_{\mathrm{sW}}^{\mathrm{F}}(\boldsymbol{R}, \boldsymbol{P}, t) \\ &= \frac{1}{\hbar^2}\int_0^\infty \mathrm{d}\tau e^{-i\hat{H}_{\mathrm{sW}}^{\mathrm{F}}t/\hbar}\mathrm{Tr}_{\mathrm{b}}([\hat{H}_{\mathrm{IcW}}^{\mathrm{F}}(t), [\hat{H}_{\mathrm{IcW}}^{\mathrm{F}}(t-\tau) \\ &\quad , e^{i\hat{H}_{\mathrm{sW}}^{\mathrm{F}}t/\hbar}\hat{\rho}_{\mathrm{sW}}^{\mathrm{F}}(t)e^{-i\hat{H}_{\mathrm{sW}}^{\mathrm{F}}t/\hbar} \otimes \hat{\rho}_{\mathrm{b}}^{\mathrm{eq}}]])e^{i\hat{H}_{\mathrm{sW}}^{\mathrm{F}}t/\hbar}\end{aligned} \tag{17}$$

Notice the similarity between the results in eqs 8 and 17. In eq 17, we have applied the Floquet theorem to make the time-dependent Hamiltonian time-independent such that we can replace every term in eq 8 by its Floquet counterpart to arrive at eq 17. The derivations for both eqs 8 and 17 follow a Redfield theory in treating the system−bath couplings, as well as a Wigner transformation in treating classical nuclear motion.

For SH, it is useful to express FR-QCLE-CME in an adiabatic Floquet basis $|\Psi_N^{\mathrm{F(ad)}}\rangle$, where $\hat{H}_{\mathrm{sW}}^{\mathrm{F}}|\Psi_N^{\mathrm{F(ad)}}\rangle = \tilde{E}_N|\Psi_N^{\mathrm{F(ad)}}\rangle$. Then the FR-QCLE-CME in eq 15 can be written as

$$\begin{aligned}\frac{\partial}{\partial t}\hat{\rho}_{\mathrm{sW}}^{\mathrm{F(ad)}}(\boldsymbol{R}, \boldsymbol{P}, t) = &-\frac{i}{\hbar}\Delta\hat{\Lambda}^{\mathrm{F}}(\boldsymbol{R})\bigcirc \hat{\rho}_{\mathrm{sW}}^{\mathrm{F(ad)}} - \sum_\alpha \frac{P_\alpha}{m_\alpha}[\hat{D}_\alpha(\boldsymbol{R}), \hat{\rho}_{\mathrm{sW}}^{\mathrm{F(ad)}}] \\ &- \frac{1}{2}\sum_\alpha\left[\hat{F}_\alpha(\boldsymbol{R}), \frac{\partial\hat{\rho}_{\mathrm{sW}}^{\mathrm{F(ad)}}}{\partial P_\alpha}\right] \\ &- \sum_\alpha \frac{P_\alpha}{m_\alpha}\frac{\partial\hat{\rho}_{\mathrm{sW}}^{\mathrm{F(ad)}}}{\partial R_\alpha} \\ &- \hat{\hat{\mathcal{L}}}_{\mathrm{bsW}}^{\mathrm{F(ad)}}(\boldsymbol{R})\hat{\rho}_{\mathrm{sW}}^{\mathrm{F(ad)}}\end{aligned} \tag{18}$$

where $\Delta\hat{\Lambda}^{\mathrm{F}}$ is the eigenvalue difference matrix of $\hat{H}_{\mathrm{sW}}^{\mathrm{F}}$ ($\Delta\Lambda_{NM}^{\mathrm{F}} = \tilde{E}_N - \tilde{E}_M$), $A\bigcirc B$ is the Hadamard product of two matrices with the same dimension, $\hat{F}^\alpha$ is the force matrix $\left(F_{NM}^\alpha \equiv -\langle\Psi_N^{\mathrm{F(ad)}}\left|\frac{\partial\hat{H}_{\mathrm{sW}}^{\mathrm{F}}}{\partial R^\alpha}\right|\Psi_M^{\mathrm{F(ad)}}\rangle\right)$, and $\hat{D}^\alpha$ is the derivative coupling matrix ($D_{NM}^\alpha \equiv F_{NM}^\alpha/(\tilde{E}_N - \tilde{E}_M)$). In the Supporting Information, we give a form of the Redfield operator $\hat{\hat{\mathcal{L}}}_{\mathrm{bsW}}^{\mathrm{F}}(\boldsymbol{R})$ both in diabatic and adiabatic representations. Next, we will use trajectory-based algorithms to solve the FR-QCLE-CME.

2.2. FR-SH Algorithm. The FR-QCLE-CME can be solved by a FR-SH algorithm. Similar to the SH proposed by Dou and Subotnik,[20] for each trajectory, we propagate the density matrix $\hat{\sigma}$ according to

$$\begin{aligned}\dot{\hat{\sigma}}^{\mathrm{F(ad)}} = &-\frac{i}{\hbar}\Delta\hat{\Lambda}^{\mathrm{F}}(\boldsymbol{R})\bigcirc\hat{\sigma}^{\mathrm{F(ad)}} - \sum_\alpha\frac{P_\alpha}{m_\alpha}[\hat{D}_\alpha(\boldsymbol{R}), \hat{\sigma}^{\mathrm{F(ad)}}] \\ &- \hat{\hat{\mathcal{L}}}_{\mathrm{bsW}}^{\mathrm{F(ad)}}(\boldsymbol{R})\hat{\sigma}^{\mathrm{F(ad)}}\end{aligned} \tag{19}$$

as well as position and momentum ($\boldsymbol{R}$ and $\boldsymbol{P}$) on the active potential surface λ

$$\dot{R}_\alpha = \frac{P_\alpha}{m_\alpha} \tag{20}$$

$$\dot{P}_\alpha = F_{\alpha(\lambda\lambda)} \tag{21}$$

In the spirit of Tully's SH, the nuclei hop among adiabatic potential energy surfaces. The total change of the population on state M is

$$\begin{aligned}\dot{\sigma}_{MM}^{\mathrm{F(ad)}} = &-\sum_{\alpha K}\frac{P_\alpha}{m_\alpha}(D_{\alpha(MK)}(\boldsymbol{R})\sigma_{KM}^{\mathrm{F(ad)}} - \sigma_{MK}^{\mathrm{F(ad)}}D_{\alpha(KM)}(\boldsymbol{R})) \\ &- \sum_{KL}\mathcal{L}_{MM,KL(\mathrm{bsW})}^{\mathrm{F(ad)}}(\boldsymbol{R})\sigma_{KL}^{\mathrm{F(ad)}}\end{aligned} \tag{22}$$

The first term on the right-hand side (rhs) of eq 22 indicates hopping due to derivative coupling D_{NM}^α. Therefore, we can define the hopping rate $k_{N\to M}^D$ caused by derivative coupling as

$$k_{N\to M}^D = \Theta\left(-2\mathrm{Re}\sum_\alpha\frac{P_\alpha}{m_\alpha}\frac{D_{\alpha(MN)}\sigma_{NM}^{\mathrm{F(ad)}}}{\sigma_{NN}^{\mathrm{F(ad)}}}\right) \tag{23}$$

where Θ function is defined as

https://doi.org/10.1021/acs.jctc.3c01263
J. Chem. Theory Comput. 2024, 20, 644−650

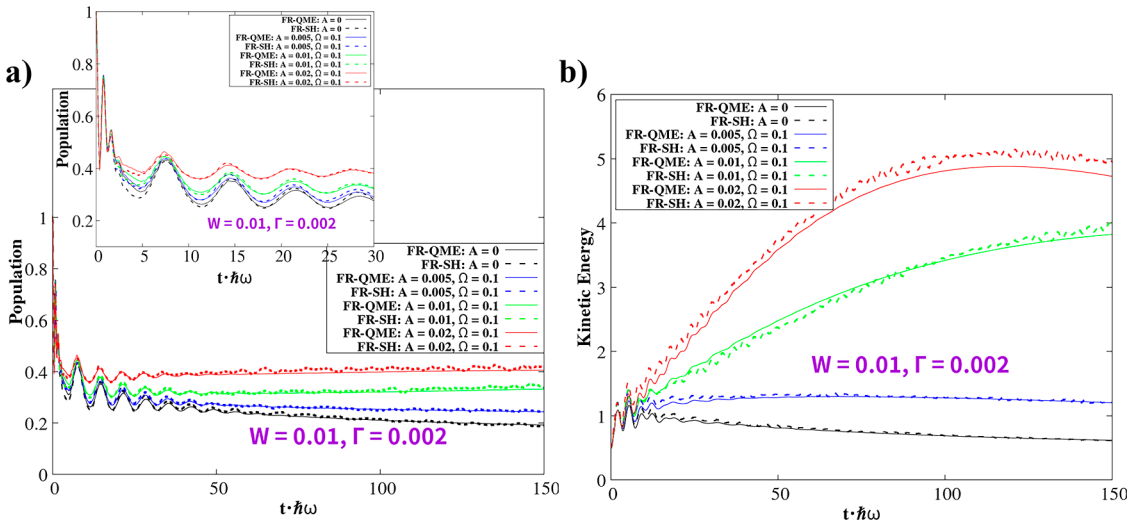

Figure 1. Diabatic electronic population on the donor $\langle \hat{d}_D^+ \hat{d}_D \rangle$ and kinetic energy as a function of time under Floquet drivings on donor−acceptor coupling. $kT = 0.01$, $\hbar\omega = 0.003$, $g = 0.0075$, $\epsilon_D = 2E_r$, $E_r = g^2/(\hbar\omega)$, $W = 0.01$, and $\Gamma = 0.002$.

$$\Theta(x) = \begin{cases} x, & (x \geq 0) \\ 0, & (x < 0) \end{cases} \tag{24}$$

The second term on the rhs of eq 22 is an extra hopping due to the molecule−metal interaction. This term has both diagonal and off-diagonal contributions

$$-\sum_{KL} \mathcal{L}^{\mathrm{F(ad)}}_{MM,KL(\mathrm{bsW})}(\boldsymbol{R})\sigma^{\mathrm{ad}}_{KL} = -\sum_{N} \mathcal{L}^{\mathrm{F(ad)}}_{MM,NN(\mathrm{bsW})}(\boldsymbol{R})\sigma^{\mathrm{ad}}_{NN} - \sum_{K\neq L} \mathcal{L}^{\mathrm{F(ad)}}_{MM,KL(\mathrm{bsW})}(\boldsymbol{R})\sigma^{\mathrm{ad}}_{KL} \tag{25}$$

Here, we employ the secular approximation to ignore the off-diagonal part, which is accurate in long-time dynamics. Such that the hopping rate caused by interactions between the system and electronic bath $k^{\mathcal{L}}_{N\to M}$ reads as

$$k^{\mathcal{L}}_{N\to M} = -\mathcal{L}^{\mathrm{F(ad)}}_{MM,NN(\mathrm{bsW})} \tag{26}$$

The details of operating such an FR-SH algorithm step by step are given in the Supporting Information.

3. RESULTS

To test our FR-SH algorithm, we used a donor−acceptor−metal model. We consider here the condition of external periodic drivings acting on the coupling strength between the donor and acceptor, namely, the case of light interacting with the transition dipole moment of the donor and acceptor. The system Hamiltonian corresponding to this case is

$$\hat{H}_{\mathrm{sW}}(x,t) = E_D(x)\hat{d}_D^+\hat{d}_D + E_A(x)\hat{d}_A^+\hat{d}_A + (W + A\sin(\Omega t))(\hat{d}_D^+\hat{d}_A + \hat{d}_A^+\hat{d}_D) + \frac{1}{2}m\omega^2x^2 + \frac{p^2}{2m} \tag{27}$$

where A is the driving amplitude and Ω is the driving frequency. We further set $E_D(x) = gx\sqrt{2m\omega/\hbar} + \epsilon_D$ and $E_A(x) = 0$. In this model, we have

$$\Gamma_{AA} = \Gamma,\ \Gamma_{DD} = \Gamma_{DA} = \Gamma_{AD} = 0 \tag{28}$$

We benchmark the FR-SH algorithm against the FR-QME in eq 13. Note that we are dealing with a four-state system in Fock space: diabatic state 1 is both donor and acceptor are unoccupied; diabatic state 2(3) is only the donor(acceptor) is occupied; and diabatic state 4 is both donor and acceptor are occupied. In FR, all these four states in Fock space will be expanded in Floquet space. Note that we need to truncate the Floquet space according to the ratio of driving amplitude A and driving frequency Ω, see details in ref 44. Briefly, the greater the $\frac{A}{\Omega}$ is, the larger the Floquet space should be. We prepared the nuclei with a Boltzmann distribution on diabatic donor states (diabatic state 2). To transfer from adiabatic to diabatic states, we follow the scheme in refs 20 and 47, such that the diabatic donor population $\langle \hat{d}_D^+\hat{d}_D \rangle$ is

$$\langle \hat{d}_D^+\hat{d}_D \rangle = \frac{1}{N_{\mathrm{traj}}}\sum_l^{N_{\mathrm{traj}}} \Big(\sum_i |U_{ai}|^2\delta_{i,\lambda^l} + \sum_{i<j} 2\mathrm{Re}(U_{ai}\sigma^{\mathrm{F}(l)}_{ij}U^*_{aj}) + \sum_i |U_{bi}|^2\delta_{i,\lambda^l} \Big) \tag{29}$$

here N_{traj} is the total number of trajectories, which is 10,000 in this study, a is an index for diabatic state 2 in which only the donor is occupied, b is an index for diabatic state 4 in which both donor and acceptor are occupied, l is an index for trajectories, and λ is the active Floquet potential energy surface. For FR-QME, we used 100 phonons to get good convergences.

Next, we investigate the dynamics of diabatic donor populations and nuclear kinetics energy. We choose three kinds of driving amplitudes: weak driving ($A = 0.005$), medium strong driving ($A = 0.01$), and strong driving ($A = 0.02$), comparing with nuclear oscillation strength ($\hbar\omega = 0.003$). All of these drivings are fast drivings that we fix a relatively large driving frequency $\Omega = 0.1$. We benchmark the FR-SH algorithm with FR-QME.

In Figure 1, we work in the regime in which W is much larger than Γ. In such a case, the FR-SH (dashed line) agrees well with FR-QME (solid line) under any drivings, for both diabatic population (Figure 1a) and kinetic energy (Figure 1b) dynamics. It is because $k^{\mathcal{L}}_{N\to M}$ (relate to Γ, which is defined in

https://doi.org/10.1021/acs.jctc.3c01263
J. Chem. Theory Comput. 2024, 20, 644−650

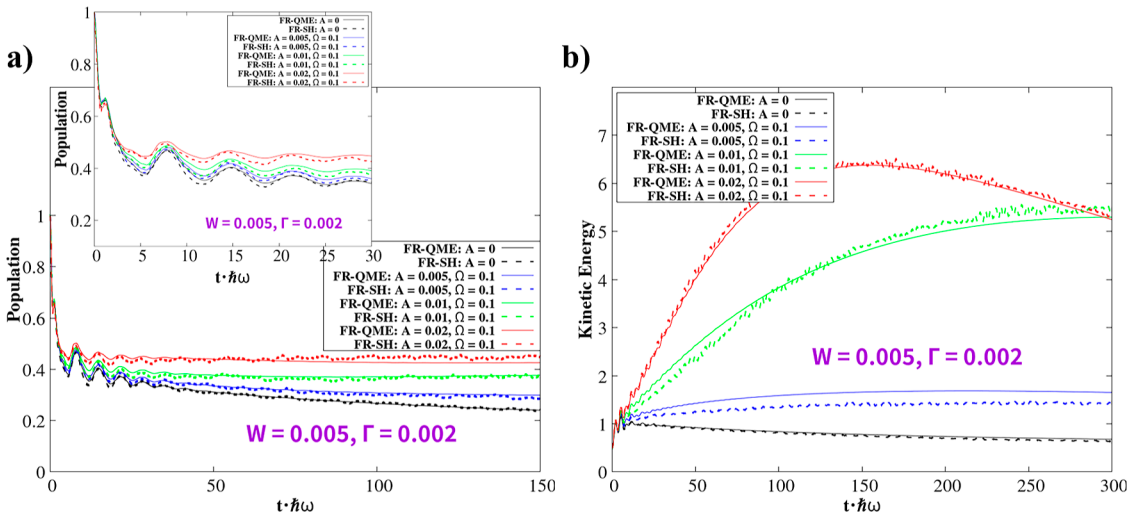

Figure 2. Diabatic electronic population on the donor $\langle \hat{d}_D^+ \hat{d}_D \rangle$ and kinetic energy as a function of time under Floquet drivings on donor−acceptor coupling. $kT = 0.01$, $\hbar\omega = 0.003$, $g = 0.0075$, $\epsilon_D = 2E_r$, $E_r = g^2/(\hbar\omega)$, $W = 0.005$, and $\Gamma = 0.002$.

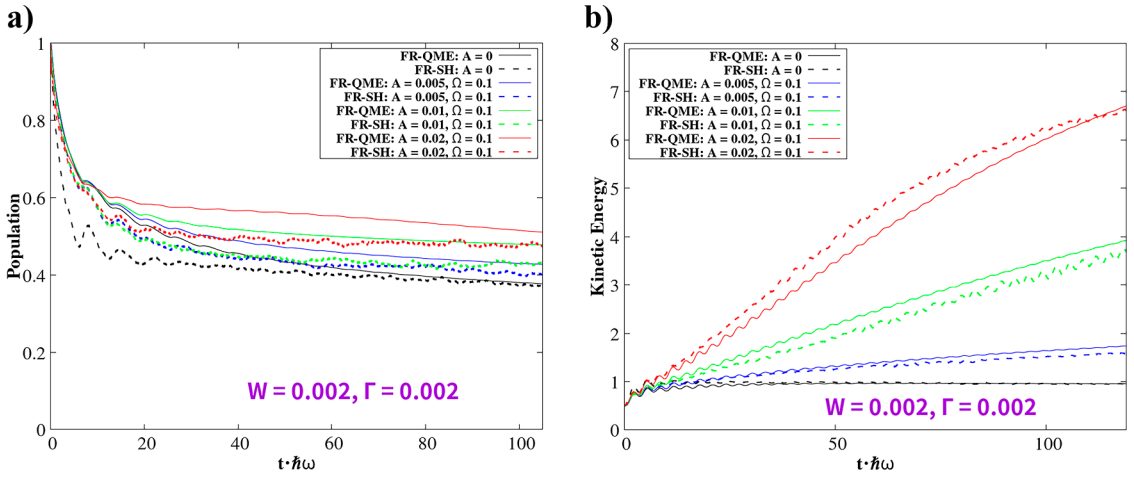

Figure 3. Diabatic electronic population on the donor $\langle \hat{d}_D^+ \hat{d}_D \rangle$ and kinetic energy as a function of time under Floquet drivings on donor−acceptor coupling. $kT = 0.01$, $\hbar\omega = 0.003$, $g = 0.0075$, $\epsilon_D = 2E_r$, $E_r = g^2/(\hbar\omega)$, $W = 0.002$, and $\Gamma = 0.002$.

eq 26) is much smaller than $k^D_{N\to M}$ (relate to W, which is defined in eq 23). That is to say, the ignorance of off-diagonal terms in hopping rates $k^{\mathcal{L}}_{N\to M}$ cannot affect dynamics in both short and long times. We can see from long-time dynamics in Figure 1a that with increasing driving amplitude A, the electronic population of the donor reaches a higher steady state. Additionally, with increasing driving amplitude, the system reaches a higher temperature as shown in Figure 1b, which is the heating effect arising from the external drivings.[44,45]

Next, we work in the regime where W is a little larger than Γ (Figure 2). In such a case, FR-SH covers the right steady state in the long-time dynamics as compared with FR-QME. However, FR-SH fails at the short-time dynamics (as shown in the inset of Figure 2a). Note that in the FR-SH method, we have applied secular approximation, which disregards the off-diagonal terms in the electronic density. Obviously, disregarding these terms can give rise to inaccurate short-time dynamics. Again, the electronic population of the donor reaches a higher steady state with increasing driving amplitude A as can be seen in Figure 2a. Also, the system reaches a higher temperature as A increases (see Figure 2b).

Finally, when W is comparable with Γ (Figure 3), we see differences between FR-SH and FR-QME under any kind of driving. In such a case, the off-diagonal terms in $k^{\mathcal{L}}_{N\to M}$ are dominant. Therefore, the secular approximated SH algorithm here cannot cover the right dynamics.[20]

Overall, our generalized FR-SH method works well under fast driving conditions when W is much larger than Γ. Note that we have exclusively studied the fast driving case with a driving frequency of $\Omega = 0.1$. In principle, the Floquet theorem can be applied to any periodic driving. That being said, when the driving frequency is small, many Floquet replicas are needed to converge the results, making the method numerically challenging.

4. CONCLUSIONS

In summary, we have proposed a generalized FR-SH algorithm to deal with the nonadiabatic dynamics near the metal surface with fast periodic drivings. In the regime where donor−acceptor coupling W is relatively larger than system−bath

https://doi.org/10.1021/acs.jctc.3c01263
J. Chem. Theory Comput. 2024, 20, 644−650

coupling Γ, FR-SH agrees well with FR-QME for both diabatic population and nuclear kinetic energy dynamics under different Floquet drivings. However, when W is comparable with Γ, FR-SH fails due to its ignorance of the off-diagonal terms in $k^{\mathcal{L}}_{N\to M}$. We see that with increasing driving amplitude A, the electronic population of the donor reaches a higher steady state, and the nuclear kinetic energy reaches a higher temperature. We expect this generalized FR-SH algorithm to be useful for modeling realistic nonadiabatic dynamics near the metal surface with periodic drivings.

■ ASSOCIATED CONTENT

Supporting Information

The Supporting Information is available free of charge at https://pubs.acs.org/doi/10.1021/acs.jctc.3c01263.

Redfield operator $\hat{\hat{\mathcal{L}}}^{\mathrm{F}}_{\mathrm{bsW}}(\boldsymbol{R})$ in either diabatic or adiabatic representation and the performance of the FR-SH algorithm step by step (PDF)

■ AUTHOR INFORMATION

Corresponding Author

Wenjie Dou − *Department of Chemistry, School of Science, Westlake University, Hangzhou, Zhejiang 310024, China; Institute of Natural Sciences, Westlake Institute for Advanced Study, Hangzhou, Zhejiang 310024, China;* orcid.org/0000-0001-5410-6183; Email: douwenjie@westlake.edu.cn

Authors

Yu Wang − *Department of Chemistry, School of Science, Westlake University, Hangzhou, Zhejiang 310024, China; Institute of Natural Sciences, Westlake Institute for Advanced Study, Hangzhou, Zhejiang 310024, China;* orcid.org/0000-0001-7278-8608

Vahid Mosallanejad − *Department of Chemistry, School of Science, Westlake University, Hangzhou, Zhejiang 310024, China; Institute of Natural Sciences, Westlake Institute for Advanced Study, Hangzhou, Zhejiang 310024, China*

Wei Liu − *Department of Chemistry, School of Science, Westlake University, Hangzhou, Zhejiang 310024, China; Institute of Natural Sciences, Westlake Institute for Advanced Study, Hangzhou, Zhejiang 310024, China;* orcid.org/0009-0006-7686-929X

Complete contact information is available at: https://pubs.acs.org/10.1021/acs.jctc.3c01263

Notes

The authors declare no competing financial interest.

■ ACKNOWLEDGMENTS

This material is based upon the work supported by the National Science Foundation of China (NSFC no. 22273075).

■ REFERENCES

(1) Subotnik, J. E.; Jain, A.; Landry, B.; Petit, A.; Ouyang, W.; Bellonzi, N. Understanding the surface hopping view of electronic transitions and decoherence. *Annu. Rev. Phys. Chem.* **2016**, *67*, 387−417.

(2) Agostini, F.; Curchod, B. F. Different flavors of nonadiabatic molecular dynamics. *Wiley Interdiscip. Rev.: Comput. Mol. Sci.* **2019**, *9*, No. e1417.

(3) Dou, W.; Subotnik, J. E. Nonadiabatic molecular dynamics at metal surfaces. *J. Phys. Chem. A* **2020**, *124*, 757−771.

(4) Cui, X.; Li, W.; Ryabchuk, P.; Junge, K.; Beller, M. Bridging homogeneous and heterogeneous catalysis by heterogeneous single-metal-site catalysts. *Nat. Catal.* **2018**, *1*, 385−397.

(5) Zhong, J.; Yang, X.; Wu, Z.; Liang, B.; Huang, Y.; Zhang, T. State of the art and perspectives in heterogeneous catalysis of CO 2 hydrogenation to methanol. *Chem. Soc. Rev.* **2020**, *49*, 1385−1413.

(6) Bavykina, A.; Kolobov, N.; Khan, I. S.; Bau, J. A.; Ramirez, A.; Gascon, J. Metal−organic frameworks in heterogeneous catalysis: recent progress, new trends, and future perspectives. *Chem. Rev.* **2020**, *120*, 8468−8535.

(7) Huber, F.; Berwanger, J.; Polesya, S.; Mankovsky, S.; Ebert, H.; Giessibl, F. J. Chemical bond formation showing a transition from physisorption to chemisorption. *Science* **2019**, *366*, 235−238.

(8) Cai, H.; Chin, Y.-H. C. Catalytic effects of chemisorbed sulfur on pyridine and cyclohexene hydrogenation on Pd and Pt clusters. *ACS Catal.* **2021**, *11*, 1684−1705.

(9) Gu, M.-W.; Peng, H. H.; Chen, I.; Chen, C. h. Tuning surface d bands with bimetallic electrodes to facilitate electron transport across molecular junctions. *Nat. Mater.* **2021**, *20*, 658−664.

(10) Liu, Y.; Qiu, X.; Soni, S.; Chiechi, R. C. Charge transport through molecular ensembles: recent progress in molecular electronics. *Chem. Phys. Rev.* **2021**, *2*, 021303.

(11) Bulla, R.; Costi, T. A.; Pruschke, T. Numerical renormalization group method for quantum impurity systems. *Rev. Mod. Phys.* **2008**, *80*, 395−450.

(12) Costi, T.; Hewson, A.; Zlatic, V. Transport coefficients of the Anderson model via the numerical renormalization group. *J. Phys.: Condens. Matter* **1994**, *6*, 2519−2558.

(13) Thoss, M.; Kondov, I.; Wang, H. Correlated electron-nuclear dynamics in ultrafast photoinduced electron-transfer reactions at dye-semiconductor interfaces. *Phys. Rev. B: Condens. Matter Mater. Phys.* **2007**, *76*, 153313.

(14) Schinabeck, C.; Erpenbeck, A.; Härtle, R.; Thoss, M. Hierarchical quantum master equation approach to electronic-vibrational coupling in nonequilibrium transport through nano-systems. *Phys. Rev. B: Condens. Matter Mater. Phys.* **2016**, *94*, 201407.

(15) Xu, M.; Liu, Y.; Song, K.; Shi, Q. A non-perturbative approach to simulate heterogeneous electron transfer dynamics: Effective mode treatment of the continuum electronic states. *J. Chem. Phys.* **2019**, *150*, 044109.

(16) Mühlbacher, L.; Rabani, E. Real-time path integral approach to nonequilibrium many-body quantum systems. *Phys. Rev. Lett.* **2008**, *100*, 176403.

(17) Dou, W.; Nitzan, A.; Subotnik, J. E. Surface hopping with a manifold of electronic states. II. Application to the many-body Anderson-Holstein model. *J. Chem. Phys.* **2015**, *142*, 084110.

(18) Dou, W.; Nitzan, A.; Subotnik, J. E. Surface hopping with a manifold of electronic states. III. Transients, broadening, and the Marcus picture. *J. Chem. Phys.* **2015**, *142*, 234106.

(19) Dou, W.; Subotnik, J. E. A many-body states picture of electronic friction: The case of multiple orbitals and multiple electronic states. *J. Chem. Phys.* **2016**, *145*, 054102.

(20) Dou, W.; Subotnik, J. E. A generalized surface hopping algorithm to model nonadiabatic dynamics near metal surfaces: The case of multiple electronic orbitals. *J. Chem. Theory Comput.* **2017**, *13*, 2430−2439.

(21) Manakov, N. L.; Ovsiannikov, V. D.; Rapoport, L. P. Atoms in a laser field. *Phys. Rep.* **1986**, *141*, 320−433.

(22) Nerush, E.; Kostyukov, I. Y.; Fedotov, A.; Narozhny, N.; Elkina, N.; Ruhl, H. Laser field absorption in self-generated electron-positron pair plasma. *Phys. Rev. Lett.* **2011**, *106*, 035001.

(23) Fülöp, J. A.; Tzortzakis, S.; Kampfrath, T. Laser-driven strong-field terahertz sources. *Adv. Opt. Mater.* **2020**, *8*, 1900681.

(24) Garcia-Vidal, F. J.; Ciuti, C.; Ebbesen, T. W. Manipulating matter by strong coupling to vacuum fields. *Science* **2021**, *373*, No. eabd0336.

(25) Orgiu, E.; George, J.; Hutchison, J.; Devaux, E.; Dayen, J.; Doudin, B.; Stellacci, F.; Genet, C.; Schachenmayer, J.; Genes, C.; et al. Conductivity in organic semiconductors hybridized with the vacuum field. *Nat. Mater.* **2015**, *14*, 1123−1129.
(26) Krainova, N.; Grede, A. J.; Tsokkou, D.; Banerji, N.; Giebink, N. C. Polaron photoconductivity in the weak and strong light-matter coupling regime. *Phys. Rev. Lett.* **2020**, *124*, 177401.
(27) Coles, D. M.; Somaschi, N.; Michetti, P.; Clark, C.; Lagoudakis, P. G.; Savvidis, P. G.; Lidzey, D. G. Polariton-mediated energy transfer between organic dyes in a strongly coupled optical microcavity. *Nat. Mater.* **2014**, *13*, 712−719.
(28) Zhong, X.; Chervy, T.; Wang, S.; George, J.; Thomas, A.; Hutchison, J. A.; Devaux, E.; Genet, C.; Ebbesen, T. W. Non-Radiative Energy Transfer Mediated by Hybrid Light-Matter States. *Angew. Chem.* **2016**, *128*, 6310−6314.
(29) Daskalakis, K.; Maier, S.; Murray, R.; Kéna-Cohen, S. Nonlinear interactions in an organic polariton condensate. *Nat. Mater.* **2014**, *13*, 271−278.
(30) Goblot, V.; Rauer, B.; Vicentini, F.; Le Boité, A.; Galopin, E.; Lemaître, A.; Le Gratiet, L.; Harouri, A.; Sagnes, I.; Ravets, S.; et al. Nonlinear Polariton Fluids in a Flatband Reveal Discrete Gap Solitons. *Phys. Rev. Lett.* **2019**, *123*, 113901.
(31) Zhao, J.; Fieramosca, A.; Bao, R.; Du, W.; Dini, K.; Su, R.; Feng, J.; Luo, Y.; San-vitto, D.; Liew, T. C.; et al. Nonlinear polariton parametric emission in an atomically thin semiconductor based microcavity. *Nat. Nanotechnol.* **2022**, *17*, 396−402.
(32) Hutchison, J. A.; Schwartz, T.; Genet, C.; Devaux, E.; Ebbesen, T. W. Modifying chemical landscapes by coupling to vacuum fields. *Angew. Chem., Int. Ed.* **2012**, *51*, 1592−1596.
(33) Herrera, F.; Spano, F. C. Cavity-controlled chemistry in molecular ensembles. *Phys. Rev. Lett.* **2016**, *116*, 238301.
(34) Mukamel, S. *Principles of Nonlinear Optical Spectroscopy*; Oxford University Press on Demand, 1999.
(35) Kohler, S. Dispersive readout: Universal theory beyond the rotating-wave approximation. *Phys. Rev. A* **2018**, *98*, 023849.
(36) Ivanov, K. L.; Mote, K. R.; Ernst, M.; Equbal, A.; Madhu, P. K. Floquet theory in magnetic resonance: Formalism and applications. *Prog. Nucl. Magn. Reson. Spectrosc.* **2021**, *126*−*127*, 17−58.
(37) Engelhardt, G.; Cao, J. Dynamical symmetries and symmetry-protected selection rules in periodically driven quantum systems. *Phys. Rev. Lett.* **2021**, *126*, 090601.
(38) Schirò, M.; Eich, F. G.; Agostini, F. Quantum−classical nonadiabatic dynamics of Floquet driven systems. *J. Chem. Phys.* **2021**, *154*, 114101.
(39) Sato, S.; De Giovannini, U.; Aeschlimann, S.; Gierz, I.; Hübener, H.; Rubio, A. Floquet states in dissipative open quantum systems. *J. Phys. B: At., Mol. Opt. Phys.* **2020**, *53*, 225601.
(40) Li, H.; Shapiro, B.; Kottos, T. Floquet scattering theory based on effective Hamiltonians of driven systems. *Phys. Rev. B: Condens. Matter Mater. Phys.* **2018**, *98*, 121101.
(41) Fiedlschuster, T.; Handt, J.; Schmidt, R. Floquet surface hopping: Laser-driven dissociation and ionization dynamics of H_2^+. *Phys. Rev. A* **2016**, *93*, 053409.
(42) Nafari Qaleh, Z.; Rezakhani, A. Enhancing energy transfer in quantum systems via periodic driving: Floquet master equations. *Phys. Rev. A* **2022**, *105*, 012208.
(43) Chen, H.-T.; Zhou, Z.; Subotnik, J. E. On the proper derivation of the Floquet-based quantum classical Liouville equation and surface hopping describing a molecule or material subject to an external field. *J. Chem. Phys.* **2020**, *153*, 044116.
(44) Wang, Y.; Dou, W. Nonadiabatic dynamics near metal surface with periodic drivings: A Floquet surface hopping algorithm. *J. Chem. Phys.* **2023**, *158*, 224109.
(45) Wang, Y.; Dou, W. Nonadiabatic dynamics near metal surfaces under Floquet engineering: Floquet electronic friction vs Floquet surface hopping. *J. Chem. Phys.* **2023**, *159*, 094103.
(46) Mosallanejad, V.; Chen, J.; Dou, W. Floquet-driven frictional effects. *Phys. Rev. B* **2023**, *107*, 184314.
(47) Landry, B. R.; Falk, M. J.; Subotnik, J. E. Communication: The correct interpretation of surface hopping trajectories: How to calculate electronic properties. *J. Chem. Phys.* **2013**, *139*, 214107.